Carbohydrate Polymers 117 (2015) 701–709

Contents lists available at ScienceDirect

Carbohydrate Polymers

journal homepage: www.elsevier.com/locate/carbpol

Homogeneous ring opening graft polymerization of ε-caprolactone onto xylan in dual polar aprotic solvents

Xueqin Zhang[a], Mingjie Chen[a,b], Chuanfu Liu[a,*], Aiping Zhang[b], Runcang Sun[a,c]

[a] State Key Laboratory of Pulp and Paper Engineering, South China University of Technology, Guangzhou 510640, PR China
[b] Institute of New Energy and New Material, Guangdong Key Laboratory for Innovative Development and Utilization of Forest Plant Germplasm, South China Agricultural University, Guangzhou 510642, PR China
[c] Beijing Key Laboratory of Lignocellulosic Chemistry, Beijing Forestry University, Beijing 100083, PR China

ARTICLE INFO

Article history:
Received 2 September 2014
Received in revised form 17 October 2014
Accepted 19 October 2014
Available online 30 October 2014

Keywords:
Xylan
Ring-opening graft polymerization
ε-Caprolactone
Dual polar aprotic solvents

ABSTRACT

Homogeneous ring-opening graft polymerization (ROGP) of ε-caprolactone (ε-CL) onto xylan was investigated in dual polar aprotic solvents, N,N-dimethylformamide/lithium chloride (DMF/LiCl), N,N-dimethylacetamide/LiCl (DMAc/LiCl), and 1-methyl-2-pyrrolidinone/LiCl (NMP/LiCl). The effects of reaction solvents, temperature, and the molar ratio of ε-CL to anhydroxylose units (AXU) on the degree of substitution (DS) of xylan-*graft*-poly(ε-caprolactone) (xylan-*g*-PCL) copolymers and the degree of polymerization (DP) of the attached PCL side chains were investigated. FT-IR and NMR analyses provided the evidence of the occurrence of ROGP reaction. The thermal stability of xylan increased upon ROGP reaction due to the increased length of PCL side chains. With the increased attachment of PCL side chains, the tensile strength and Young's modulus of the films decreased, whereas the elongation at break increased. Scanning electron microscopy (SEM) and atomic force microscopy (AFM) observations provided the evidences of the increased film properties due to the attachment of PCL side chains.

1. Introduction

Recently, an increased interest has been paid on the research of macromolecular materials based on natural lignocellulosic resources (Saha, 2003), including cellulose, hemicelluloses and lignin. These readily available biopolymers are nontoxic, renewable, biodegradable and show peculiar and distinguished physicochemical properties (Wang et al., 2012) and could be used to compensate for the shortage of petroleum-based products and solve the environmental problems (Williamson, Armentrout, Porter, & McCormick, 1998).

Hemicelluloses, the second most common polysaccharides, account for about one third of lignocellulosic biomass. The structural features of hemicelluloses is resemble to cellulose only in nominal (Saha, 2003). Hemicelluloses are branched and heterogeneous polymers of xylans, mannans, glucans and xyloglucans, with low degree of polymerization (DP) typically between 80 and 200 (Belmokaddem, Pinel, Huber, Petit Conil, & Da Silva Perez, 2011; Fundador, Enomoto-Rogers, Takemura, & Iwata, 2012). Xylan is the most abundant hemicelluloses, consisting of β-(1,4)-D-xylopyranosyl backbone with side groups on the C-2 or C-3 position (Hansen & Plackett, 2008; Sun & Tomkinson, 2002; Sun, Fang, & Tomkinson, 2000). With inherent low molecular weight, heterogeneous structure and hydrophilicity, research in the field of hemicelluloses was neglected and limited. Chemical modification is an efficient way to compensate the drawbacks of hemicelluloses as desired macromolecules (Sun et al., 2000). Among them, ring-opening graft polymerization (ROGP) is one of the commonly used techniques to synthetize polymers with controlled molecular weight and tailored properties from cyclic monomers (Carlmark, Larsson, & Malmström, 2012; El Seoud, Marson, Ciacco, & Frollini, 2000), which could be one of the ideal pathways for the modification of polysaccharides (Carlmark et al., 2012; Malmstrom & Carlmark, 2012). The efficiency of ROGP reaction onto hemicelluloses depends on: (1) an effective monomer utilized to be grafted onto hemicelluloses; (2) a good homogeneous solvent system for hemicelluloses.

Cyclic monomers, lactones and lactides, have attracted considerable attention to synthesize biomaterials with excellent biodegradability and biocompatibility. Among them, poly(ε-caprolactone) (PCL) is especially interesting for its applications due to a slower rate of degradation than poly(lactic acid) (PLA)

* Corresponding author. Tel.: +86 20 87111735; fax: +86 20 87111861.
E-mail address: chfliu@scut.edu.cn (C. Liu).

http://dx.doi.org/10.1016/j.carbpol.2014.10.061
0144-8617/

(Lönnberg et al., 2006; Marianne Labet, 2011). PCL is a semi-crystalline polymer with a low glass transition temperature (about −60 °C) and melting point (ranging between 59 and 64 °C), which depends on its crystalline nature of PCL (Sinha, Bansal, Kaushik, Kumria, & Trehan, 2004). Commonly, PCL is prepared by the ROGP reaction of ε-caprolactone (ε-CL) catalyzed with 4-dimethylaminopyridine (DMAP), stannous octoate ($Sn(Oct)_2$), and lithium chloride (LiCl) (Carlmark et al., 2012; Guo, Wang, Shen, Shu, & Sun, 2013; Xie et al., 1999). Among those catalysts, LiCl is very economic and almost nontoxic compared with $Sn(Oct)_2$ and DMAP (Xie et al., 1999).

Very recently, LiCl in dimethyl sulfoxide (DMSO), N,N-dimethylacetamide (DMAc), N,N-dimethylformamide (DMF) or 1-methyl-2-pyrrolidinone (NMP) has been found to dissolve cellulose and chitin, which allows a variety of uniform reactions to be achieved under homogeneous conditions (Gross, Bell, & Chu, 2013; Williamson et al., 1998). These solvents were reported to be extremely stable without degradation effect on polysaccharides (Dupont, 2003). Cellulose could be dissolved up to 10–15 wt% with solubility proportional to LiCl concentration of 1–10 wt% (Dupont, 2003; Gross et al., 2013; Takaragi, Minoda, Miyamoto, Liu, & Zhang, 1999). The solubility of cellulose in LiCl/amide solvent was significantly higher than that in other salt/amide solvent like lithium bromide (LiBr) (Striegel, 1997). "Grafting from" of PCL polymers to various substrates has been widely investigated, such as cellulose, cellulose derivatives, starch, chitosan, etc. (Habibi, Goffin, Schiltz, Duquesne, & Dubois, 2008). In our previous research, the xylan-*g*-PCL copolymers have been achieved in DMSO/LiCl without additional catalysts (Zhang, Chen, Liu, & Sun, 2014). However, the degree of substitution (DS) of copolymers ranged from 0.03 to 0.39, and the DP of the PCL side chains was only one. The attachment of PCL side chains onto xylan with increased DS and DP is crucial for efficient utilization of lignocellulosic biomass. In the present study, three kinds of dual polar aprotic solvents DMF/LiCl, DMAc/LiCl, and NMP/LiCl were used as solvent, reaction media and catalyst for homogeneous ROGP of ε-CL onto xylan to explore the possibility of the attachment of increased PCL side chains. The effects of reaction parameters including the reaction system, reaction temperature, and the molar ratio of ε-CL to anhydroxylose units (AXU) were comparatively investigated. The physico-chemical properties of xylan derivatives were characterized with FT-IR, ^{1}H NMR, ^{1}H–^{1}H COSY, ^{13}C NMR, ^{1}H–^{13}C HSQC, ^{1}H–^{13}C HMBC, and thermal analysis. The film-forming properties of xylan derivatives were also investigated with the surface morphologies of the films observed with scanning electron microscopy (SEM) and atomic force microscopy (AFM) as well as the mechanical properties.

2. Materials and methods

2.1. Materials

Xylan with a purity of 85% was purchased from Yuan-Ye Biological Technology Co., Ltd. (Shanghai, China). The molecular weight (Mw) of xylan was 49,027 g mol^{-1}, determined by GPC using a PL aquagel-OH 50 column according to the published method (Sun, Li, Yuan, Xu, & Sun, 2012). The commercial PCL homopolymer with average Mn 10,000 was purchased from Aladdin Reagent Co. (Shanghai, China). DMAc, DMF, and NMP were purchased from Sigma–Aldrich Co., LLC (Shanghai, China). LiCl with a purity of 97% was provided by Kermel Chemical Agent Co., Ltd. (Tianjin, China). ε-CL with 99.5% purity from Aladdin Reagent Co. was dried over CaH_2 and subsequently distilled under reduced pressure before use. Other chemicals were of analytical-reagent grade and directly used without further purification.

Table 1
Detailed structural factors of xylan-*g*-PCL copolymers obtained under various conditions.

Sample No	Temp (°C)	ε-CL/AXU	Solvent	Time (h)	DS[a]	DP[b]
1	80	8:1	DMF/LiCl	24	0.06	1.00
2	90	8:1	DMF/LiCl	24	0.07	1.00
3	100	8:1	DMF/LiCl	24	0.10	1.00
4	110	8:1	DMF/LiCl	24	0.25	1.06
5	120	8:1	DMF/LiCl	24	0.39	1.19
6	80	8:1	DMAc/LiCl	24	–	–
7	90	8:1	DMAc/LiCl	24	0.05	1.00
8	100	8:1	DMAc/LiCl	24	0.11	1.03
9	110	8:1	DMAc/LiCl	24	0.15	1.08
10	120	8:1	DMAc/LiCl	24	0.18	1.08
11	80	8:1	NMP/LiCl	24	0.04	1.00
12	90	8:1	NMP/LiCl	24	0.06	1.00
13	100	8:1	NMP/LiCl	24	0.10	1.07
14	110	8:1	NMP/LiCl	24	0.22	1.25
15	120	8:1	NMP/LiCl	24	0.25	1.54
16	100	1:1	DMF/LiCl	24	0.03	1.00
17	100	4:1	DMF/LiCl	24	0.05	1.00
18	100	12:1	DMF/LiCl	24	0.13	1.00
19	100	20:1	DMF/LiCl	24	0.12	1.00
20	100	1:1	DMAc/LiCl	24	0.01	1.00
21	100	4:1	DMAc/LiCl	24	0.07	1.00
22	100	12:1	DMAc/LiCl	24	0.24	1.26
23	100	20:1	DMAc/LiCl	24	0.52	1.54
24	100	1:1	NMP/LiCl	24	–	–
25	100	4:1	NMP/LiCl	24	0.06	1.00
26	100	12:1	NMP/LiCl	24	0.14	1.25
27	100	20:1	NMP/LiCl	24	0.55	1.53

[a] The degree of substitution of xylan-*g*-PCL copolymers, calculated by ^{1}H NMR.
[b] The degree of polymerization of PCL side chains attached onto xylan, calculated by ^{1}H NMR.

2.2. Homogeneous preparation of xylan-g-PCL copolymers in different solvent systems

The preparation of xylan-*g*-PCL copolymers was performed in dual polar aprotic solvent systems including DMF/LiCl, DMAc/LiCl, and NMP/LiCl under the conditions in Table 1 according to the following procedure: dry xylan (0.33 g, 5 mmol of hydroxyl group in xylan) was added to 20 mL solvent systems (6 wt% LiCl) in a 50 mL dried three-neck flask. The mixture was agitated with magnetic stirring at 80 °C for about 2 h under the protection of nitrogen to achieve a homogenous solution. Then to the xylan solution, ε-CL was introduced at the required temperature. The ROGP reaction was carried out under the protection of nitrogen with magnetic stirring for 24 h. After the required time, the resulting solution was cooled to room temperature. After precipitation into 150 mL ethanol, the solid residues were filtered out and thoroughly washed with ethanol. The products were suspended in dichloromethane with magnetic agitation at room temperature for 24 h (thrice, total 72 h) to remove PCL homopolymers. The solid residues were filtered out, dried in vacuum at 60 °C for 48 h and stored away from moisture, heat and light.

2.3. Film preparation

The prepared xylan-*g*-PCL copolymers (0.25 g) were dissolved in 10 mL of DMF at room temperature with magnetic stirring. Then, the mixtures were cast into polystyrene dish to form wet films. The films were dried in an oven at 50 °C for 12 h and stored in plastic bags for characterization.

2.4. Characterization

FT-IR spectra of unmodified xylan and xylan-*g*-PCL copolymers were recorded on a Bruker spectrophotometer (Tensor 27,

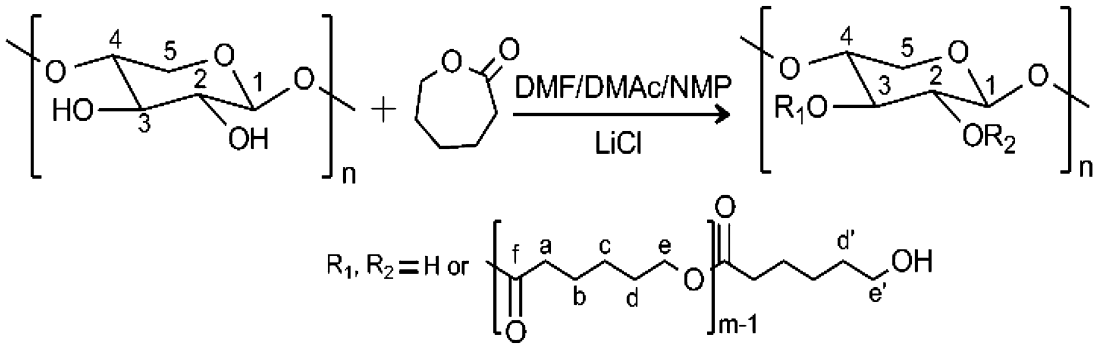

Fig. 1. The ring-opening graft polymerization of PCL onto xylan in dual polar aprotic solvents.

Germany) from a KBr disc containing 1% (w/w) finely ground samples in the range 4000–400 cm^{-1}.

The ^{1}H NMR, ^{1}H–^{1}H COSY, ^{13}C NMR, ^{1}H–^{13}C HSQC and ^{1}H–^{13}C HMBC spectra of xylan-*g*-PCL copolymers and the commercial PCL homopolymer were recorded from 40 mg samples in 0.5 mL DMSO-d_6 on a Bruker Avance III 600M spectrometer (Germany) with a 5 mm multinuclear probe. For ^{1}H NMR analysis, the detailed collecting and processing parameters were as follows: number of scans, 16; receiver gain, 252; acquisition time, 4.0894 s; relaxation delay, 2.0 s; pulse width, 11.0 s; spectrometer frequency, 600.13 MHz; and spectral width, 8012.8 Hz. For ^{1}H–^{1}H COSY analysis, the detailed collecting and processing parameters were as follows: number of scans, 16; receiver gain, 20; acquisition time, 0.3277 s; relaxation delay, 1.8 s; pulse width, 11.0 s; spectrometer frequency, 600.13/600.13 MHz; and spectral width, 3125.0/3125.0 Hz. For ^{13}C NMR analysis, the detailed collecting and processing parameters were as follows: number of scans, 2770; receiver gain, 187; acquisition time, 0.9088 s; relaxation delay, 2.0 s; pulse width, 12.0 s; spectrometer frequency, 150.91 MHz; and spectral width, 36,057.7 Hz. For HSQC analysis, the detailed collecting and processing parameters were as follows: number of scans, 32; receiver gain, 187; acquisition time, 0.1843 s; relaxation delay, 1.5 s; pulse width, 11.0 s; spectrometer frequency, 600.17/150.91 MHz; and spectral width, 5555.6/21,097.0 Hz. For HMBC analysis, number of scans, 96; receiver gain, 187; acquisition time, 0.2540 s; relaxation delay, 1.8996 s; pulse width, 11.0 s; spectrometer frequency, 600.17/150.91 MHz; and spectral width, 4032.3/33,557.0 Hz. The DS and the degree of polymerization (DP) of xylan-*g*-PCL copolymers were calculated from the integration of the resonances assigned to characteristic signals in ^{1}H NMR spectra.

The thermal stability of the samples was performed by using themogravimetric analysis (TGA) and derivative thermogravimetry (DTG) using a Q500 theromgravimetric analyzer (TA Instruments, USA). The apparatus was continually flushed with nitrogen. The sample between 9 and 11 mg was heated from 30 °C to 600 °C at a heating rate of 10 °C/min.

The surface morphology was examined by SEM on a field emission microscopy (LEO 1530 VP, LEO, Germany) and by AFM (Nanoscope III, Veeco Co. Ltd.). The samples of SEM were prepared by casting few solids onto a mica sheet followed by gold-plating. AFM scanning was conducted at four locations on each sample. Topographic (height) and phase images were recorded in tapping mode under ambient air.

The tensile strength of the prepared xylan-*g*-PCL copolymer films was determined from rectangular specimens (15 mm × 10 mm) on an Instron Universal Testing Machine 5565 fitted with a 100 N load cell at 23 °C with 50% RH.

3. Results and discussion

3.1. Effects of reaction parameters on the attachment of PCL onto xylan

Very recently, various polar aprotic solvent systems containing LiCl were found to dissolve polysaccharides and be a powerful solvent and suitable reaction medium for cellulose utilization (Dupont, 2003; Edgar, Arnold, Blount, Lawniczak, & Lowman, 1995; Stryuk, Eckelt, & Wolf, 2005). In this study, three kinds of dual aprotic solvents, including DMF/LiCl, DMAc/LiCl and NMP/LiCl, were investigated as solvents and reaction media to attach PCL onto xylan. Fig. 1 illustrates the ROGP reaction of ε-CL with the hydroxyl groups on the backbone of xylan in DMF/LiCl, DMAc/LiCl and NMP/LiCl. The effects of reaction parameters including the reaction media, reaction temperature and the molar ratio of ε-CL/AXU on the attachment of PCL onto xylan were investigated, as listed in Table 1.

As shown in Table 1, an increase of reaction temperature from 80 to 120 °C in DMF/LiCl resulted in an increase in DS from 0.06 to 0.39, while the DP of the PCL side chains was only slightly higher than 1.00 (1.19 at 120 °C). Keeping reaction temperature at 100 °C, with the improvement of the molar ratio of ε-CL to AXU from 1:1 to 20:1, the DS was only marginally improved from 0.03 to 0.12 and the DP was constant at 1.00, which suggested that only one ε-CL was attached onto xylan in DMF/LiCl at 100 °C. The low attachment of PCL onto xylan was probably due to the branched structure. The similar results were also reported in our previously research in DMSO/LiCl system (Zhang et al., 2014).

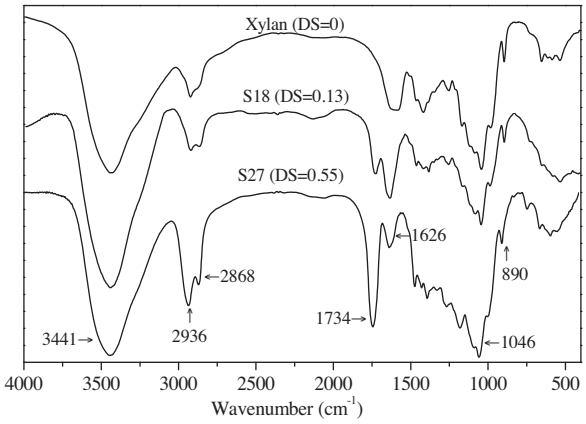

Fig. 2. FT-IR spectra of unmodified xylan, xylan-*g*-PCL copolymers samples 18 and 27.

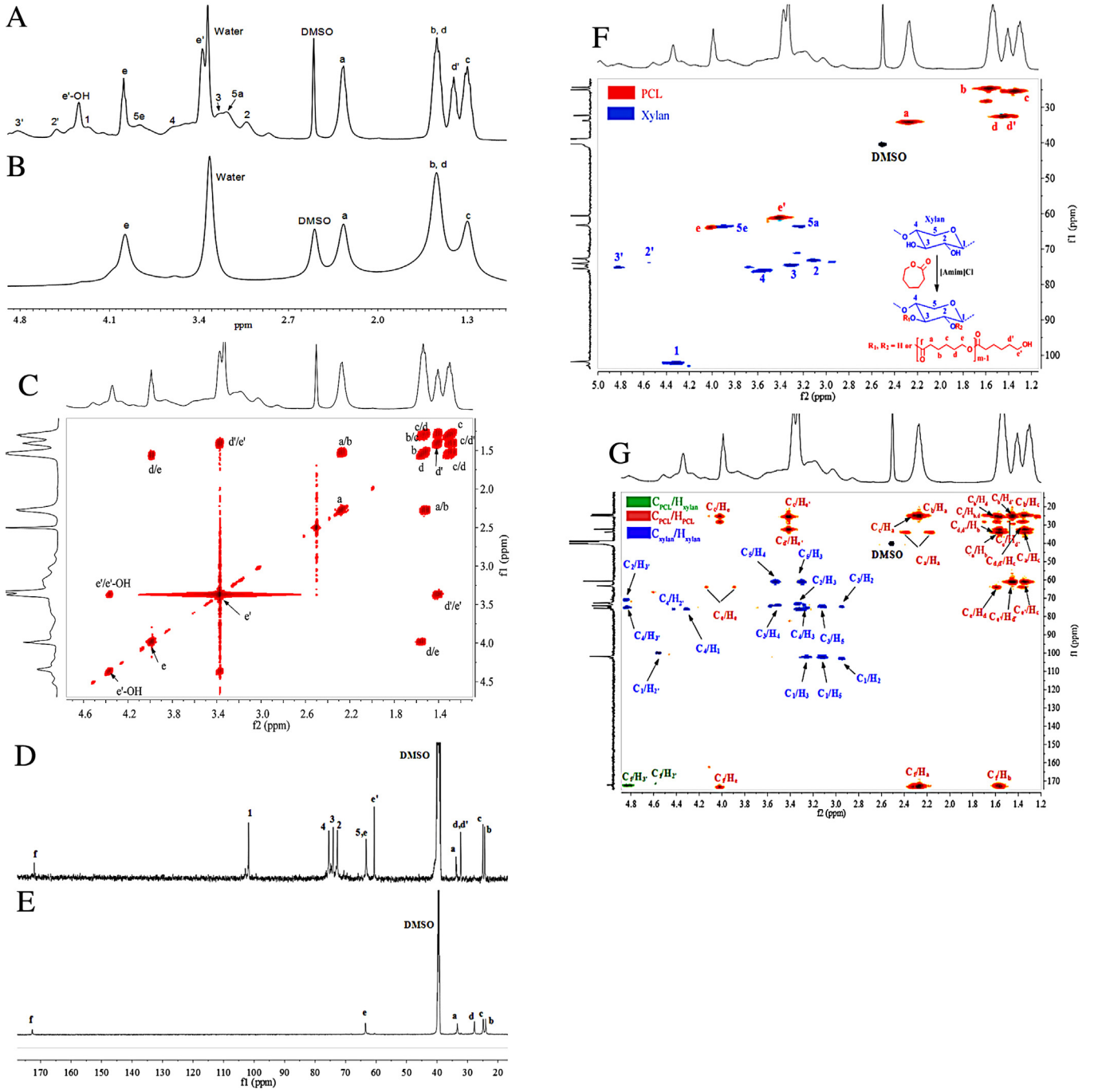

Fig. 3. ^{1}H NMR, ^{1}H–^{1}H COSY, ^{13}C NMR, ^{1}H–^{13}C HSQC and HMBC spectra of xylan-*g*-PCL copolymer sample 27 (A, C, D, F, G) and the commercial PCL homopolymer (B, E). (For interpretation of the references to color in the text, the reader is referred to the web version of this article.)

The ROGP reaction also occurred in DMAc/LiCl system and the xylan-*g*-PCL copolymers with low DS 0.05–0.18 and low DP 1.00–0.08 were obtained from 90 to 120 °C. Comparatively, the efficiency of ROGP reaction in DMAc/LiCl was lower than in DMF/LiCl, and the reaction hardly occurred even at 80 °C. The difference was probably due to the relatively slightly higher polarity of DMF. Unexpectedly, an increase of the molar ratio of ε-CL to AXU from 1:1 to 20:1 resulted in the enhancement of DS from 0.01 to 0.52 and DP from 1.00 to 1.54. It seemed that the ROGP reaction more easily occurred at high concentration of the reactant ε-CL. Similarly, in NMP/LiCl system, the reaction hardly occurred at the molar ratio of ε-CL to AXU 1:1, while with the improvement of the molar ratio of ε-CL to AXU from 4:1 to 20:1, the DS and DP was enhanced from 0.06 to 0.55 and 1.00 to 1.53, respectively. Comparatively, at lower molar ratio of ε-CL to AXU, the efficiency of ROGP reaction in the three dual polar aprotic solvent systems followed the order: DMF/LiCl > NMP/LiCl > DMAc/LiCl; however, at higher molar ratio of ε-CL to AXU, the efficiency of ROGP reaction followed the order: DMF/LiCl < NMP/LiCl < DMAc/LiCl. The changed reaction efficiency in the systems was still unclear. Under the given conditions, the DS and DP of xylan-*g*-PCL copolymers ranged 0.03–0.39 and 1.00–1.19 in DMF/LiCl, 0.01–0.52 and 1.00–1.54 in DMAc/LiCl, and 0.04–0.55 and 1.00–1.54 in NMP/LiCl, respectively.

3.2. FT-IR

Fig. 2 illustrates the FT-IR spectra of unmodified xylan, and xylan-*g*-PCL copolymer samples 18, 23 and 27. The bands at 3441, 2936, 1626, 1046 and 890 cm^{-1} in the spectrum of unmodified xylan were previously reported (Cao, Sun, Peng, Zhong, & Sun, 2013; Fundador et al., 2012). Comparatively, two new absorbances appeared at 2868 and 1734 cm^{-1} in the FT-IR spectra of xylan-*g*-PCL copolymers. The former band is attributed to CH_2 stretching and the latter relates to C=O stretching in ester (Labet & Thielemans, 2011). The intensities of these two new bands increased with the increased DS, which indicated the introduction of aliphatic ester group after modification, suggesting the occurrence of ROGP reaction of ε-CL onto xylan (Labet & Thielemans, 2011).

3.3. ^1H NMR, ^1H–^1H COSY, ^{13}C NMR, ^1H–^{13}C HSQC and ^1H–^{13}C HMBC spectra

The structures of xylan, xylan-*g*-PCL copolymers and the commercial PCL homopolymer were comparatively studied with ^1H NMR, ^1H–^1H COSY, and ^{13}C NMR analyses, as illustrated in Fig. 3.

In Fig. 3A, the proton signals at 3.02, 3.13, 3.25, 3.49, 3.85 and 4.26 ppm are assigned to H-2, H-5a, H-3, H-4, H-5e, and H-1 of AXU in xylan, and those in the range of 4.95–5.41 ppm relate to the protons from the hydroxyl groups in AXU (Cao et al., 2013). The signals at 3.95, 3.37, 2.27, 1.54, 1.41 and 1.30 ppm are assigned to the methylene protons at e (repeating unit), e′ (end unit), a, b and d, d′, and c positions, respectively, in the attached PCL side chains (Wang et al., 2013). The hydroxyl group at the end of PCL side chains (—CH_2O<u>H</u>, e′-OH) exhibited the proton signal at 4.34 ppm. Comparatively, in the ^1H NMR spectrum of the commercial PCL homopolymer in Fig. 3B, the methylene protons at c, b, d, a and e positions in repeating units of PCL gave the signals at 1.30, 1.54, 1.54, 2.27 and 3.90 ppm, respectively (He et al., 2007; Xu, Kennedy, & Liu, 2008). In addition, the signals at 4.51 and 4.82 ppm are associated with the protons at substituted C-2 and C-3 positions, respectively, confirming the attachment of PCL on C-2 and C-3 positions in AXU.

To confirm the correct assignment of the primary proton signals of the attached PCL side chains, the ^1H–^1H COSY spectrum of xylan-*g*-PCL copolymer sample 27 was collected and is illustrated in Fig. 3C. To clearly show the cross-correlations of the protons on the attached PCL side chains, the spectrum is illustrated at higher contour level and as a result the primary signals and their cross-correlations in AXU are not shown. The strong cross-correlations for a/b, b/c, c/d′, d′/e′, e′/e′-OH in PCL side chains were clearly observed, which were previously reported (Zhang et al., 2014). As excepted, another two strong cross-correlations at δ_H/δ_H of 3.99/1.54 and 1.54/3.99 for d/e indicated the high content of the PCL side chains, suggesting the increased length of PCL side chains compared with those prepared in DMSO/LiCl system (Zhang et al., 2014). The methylene proton signals at b and d positions in PCL repeating unit were overlapped at 1.54 ppm, which could be confirmed by the presence of strong cross-correlations for d/e. Due to the increased length of PCL side chains, it was necessary to further calculate the DS of xylan-*g*-PCL copolymers and DP of the attached PCL side chains.

Theoretically, there are the equal quantities of overall methylene protons at different positions from a to e in the attached PCL chains including the repeating units and the end units due to the special structure of ε-CL. The DP of the attached PCL side chains could be estimated from the different signals of e positions at repeating units (e) and end units (e′). The DS of xylan-*g*-PCL copolymers could be estimated from the quantities of PCL side chains on each AXU. Therefore, the DS and DP was calculated from the

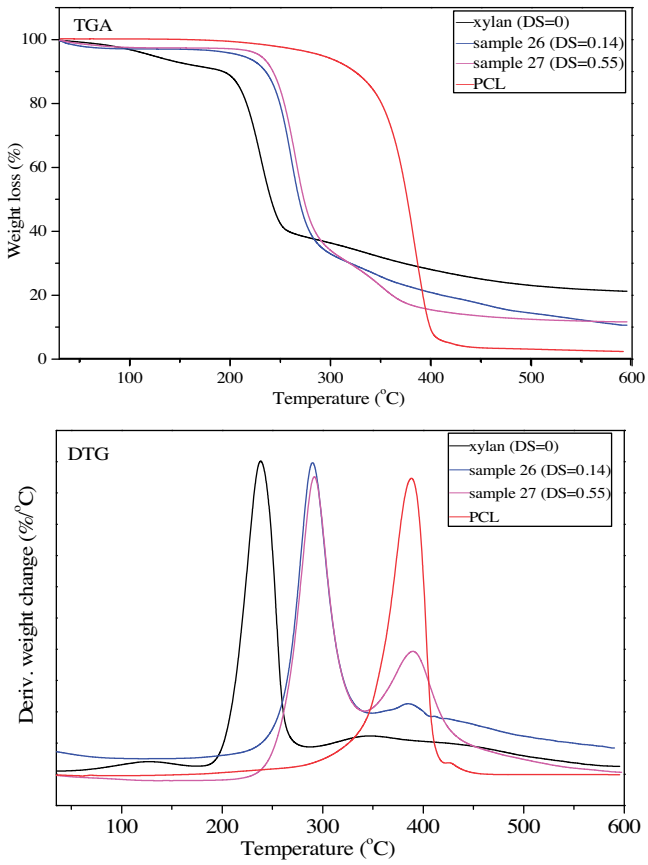

Fig. 4. TGA/DTG curves of regenerated xylan, xylan-*g*-PCL copolymers (samples 26 and 27), and the commercial PCL homopolymer.

integral area of the resonances for the corresponding protons according to the following equation:

$$DS = \frac{CL_{Terminal}}{AXU} = \frac{I_{e'}/2}{I_{H_4}} = \frac{I_{d'}/2}{I_{H_4}}$$

$$DP = \frac{CL_{Total}}{CL_{Terminal}} = \frac{I_{(e+e')}}{I_{e'}} = \frac{I_a}{I_{d'}}$$

where DS is the degree of substitution of PCL, DP is the degree of polymerization of PCL, AXU is anhydroxylose unit, $CL_{Terminal}$ is the end unit of PCL, CL_{Total} is the total units of PCL, 2 is two protons

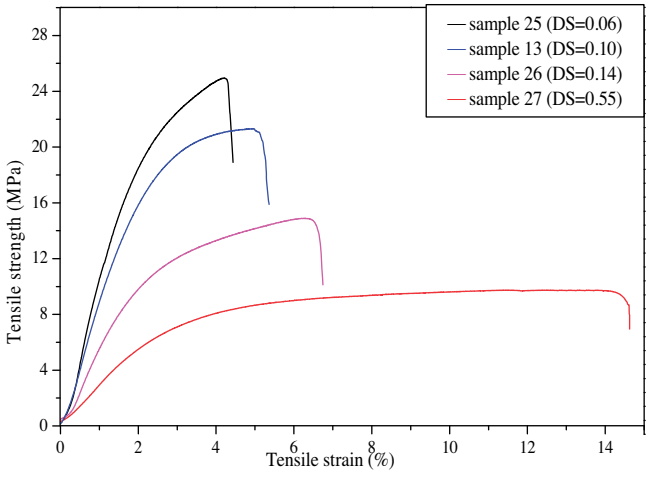

Fig. 5. Strain–stress curves of xylan-*g*-PCL films.

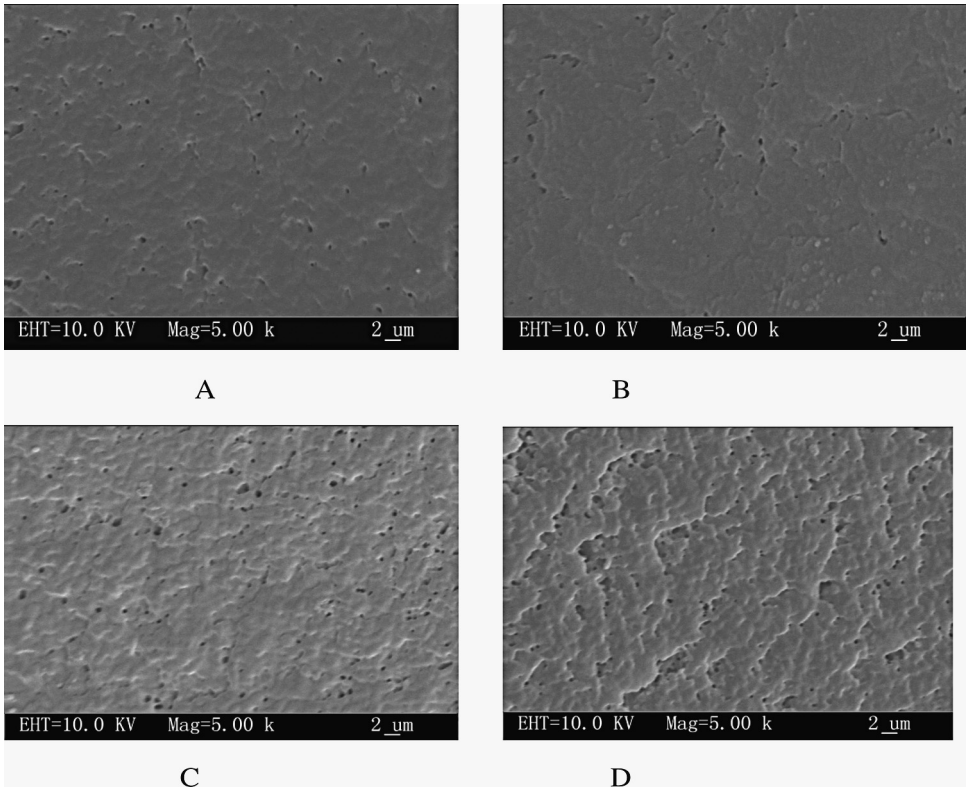

Fig. 6. SEM images of the films prepared from xylan-*g*-PCL samples 25 (A, DS 0.06), 13 (B, DS 0.10), 26 (C, DS 0.14) and 27 (D, DS 0.55).

in each methylene group, I_e, $I_{e'}$ $I_{d'}$ and I_a are the integral area of the resonances of the corresponding methylene protons at e, e′, d′ and a positions of PCL, and I_{H4} is the integral area of the resonance assigned to H_4 of AXU.

The DS and DP values estimated from ^{1}H NMR are listed in Table 1. The results indicated that the xylan derivatives with DS 0.01–0.55 and DP 1.00–1.54 were obtained under the selected conditions.

The ^{13}C NMR spectra of xylan-*g*-PCL copolymer sample 27 and the commercial PCL homopolymer are shown in Fig. 3D and E. In Fig. 3D, the five major signals at 102.1, 75.8, 74.5, 73.2 and 63.7 ppm are assigned to C-1, C-4, C-3, C-2 and C-5 of AXU in xylan, respectively (Fundador et al., 2012). The signals at 33.7, 24.5, 25.1, 32.3, and 60.6 ppm correspond to the methylene carbons of a, b, c, d, and e positions, respectively, in the PCL side chains, and the signal at 172.1 ppm is attributed to the carbonyl at f position. These carbon signals indicated the successful attachment of PCL onto xylan. Comparatively, the primary signals at 23.8, 24.8, 27.7, 33.2, 63.4 and 172.3 ppm in Fig. 3E are assigned to b, c, d, a, e and f in the commercial PCL homopolymer (Xu et al., 2008), indicating the changed chemical shift with increased length of the PCL chains.

HSQC provides detailed information of signals overlapped in ^{1}H- and ^{13}C-NMR spectra, and could be applied for qualitative and quantitative analysis of chemical structure. Fig. 3F illustrates the HSQC spectrum of xylan-*g*-PCL copolymer sample 27, and the primary correlations from xylan and PCL side chains are exhibited in Blue and Red colour, respectively. To exhibit the primary correlations both unsubstituted and substituted, the spectrum is illustrated at a relatively low contour level. The strong correlations at δ_C/δ_H 33.8/2.28, 24.1/1.54, 25.4/1.32, 32.6/1.39, 32.6/1.53, 60.4/3.38 and 63.3/3.99 ppm are associated with C_a/H_a, C_b/H_b, C_c/H_c, $C_{d'}/H_{d'}$, C_d/H_d, $C_{e'}/H_{e'}$ and C_e/H_e, respectively. The presence of these signals indicated that the PCL side chains were successfully attached onto xylan, because the PCL homopolymers have been removed by thorough extraction in dichloromethane for 72 h. In addition, the strong correlations at δ_C/δ_H 102.1/4.33, 72.6/3.05, 74.4/3.27, 75.5/3.54, 63.3/3.86, and 63.2/3.22 ppm are attributed to C_1/H_1, C_2/H_2, C_3/H_3, C_4/H_4, C_{5e}/H_{5e} and C_{5a}/H_{5a} in AXU of xylan, respectively. More importantly, the correlations at δ_C/δ_H 73.7/4.55 and 75.1/4.83 for substituted C_2/H_2 and C_3/H_3 (2′ and 3′, respectively), indicating the ROGP reactions occurred at C_2 and C_3 positions. Clearly, more PCL side chains were attached to C_3 position than to C_2 position. The integrated resonances for substituted and unsubstituted C_2/H_2 and C_3/H_3 indicated that 13.04% and 86.96% of PCL side chains were attached to C_2 and C_3 positions of AXU, respectively.

To further confirm the ROGP reaction and the assignment of the primary signals of xylan-*g*-PCL copolymers, the HMBC spectrum of xylan-*g*-PCL copolymer sample 27 is showed in Fig. 3G. In general, HMBC could give correlations between carbons and protons that are separated by two, three, and, sometimes in conjugated systems, four bonds. In Fig. 3G, the primary correlations from xylan backbone and PCL side chain are illustrated in Blue and Red colour, respectively, while the cross-correlations between xylan and PCL side chains are in Green colour. Expectedly, the presence of the Green correlations at δ_C/δ_H 173.3/4.81 ($C_f/H_{3'}$) and 173.3/4.55 ($C_f/H_{2'}$) ppm for the cross-correlations between carbonyl carbon (C=O, f carbon) in PCL side chains and the protons at the substituted C_3 and C_2 positions (3′ and 2′ protons, respectively) confirmed the chemical bonding between PCL side chain and xylan, providing the direct evidence of the attachment of PCL onto xylan at C_3 and C_2 positions. Clearly, more PCL side chains were attached to C_3 position than to C_2 position, corresponding to the results from HSQC. In addition, the correlations at δ_C/δ_H 173.3/4.02 (C_f/H_e), 172.1/2.27 (C_f/H_a), and 172.1/1.55 ppm (C_f/H_b) are attributed to the cross-correlations between carbonyl carbon and methylene protons in PCL chains. The strong cross-correlation of C_f/H_e implied that DP of the attached PCL side chains was higher than 1. These observations were in

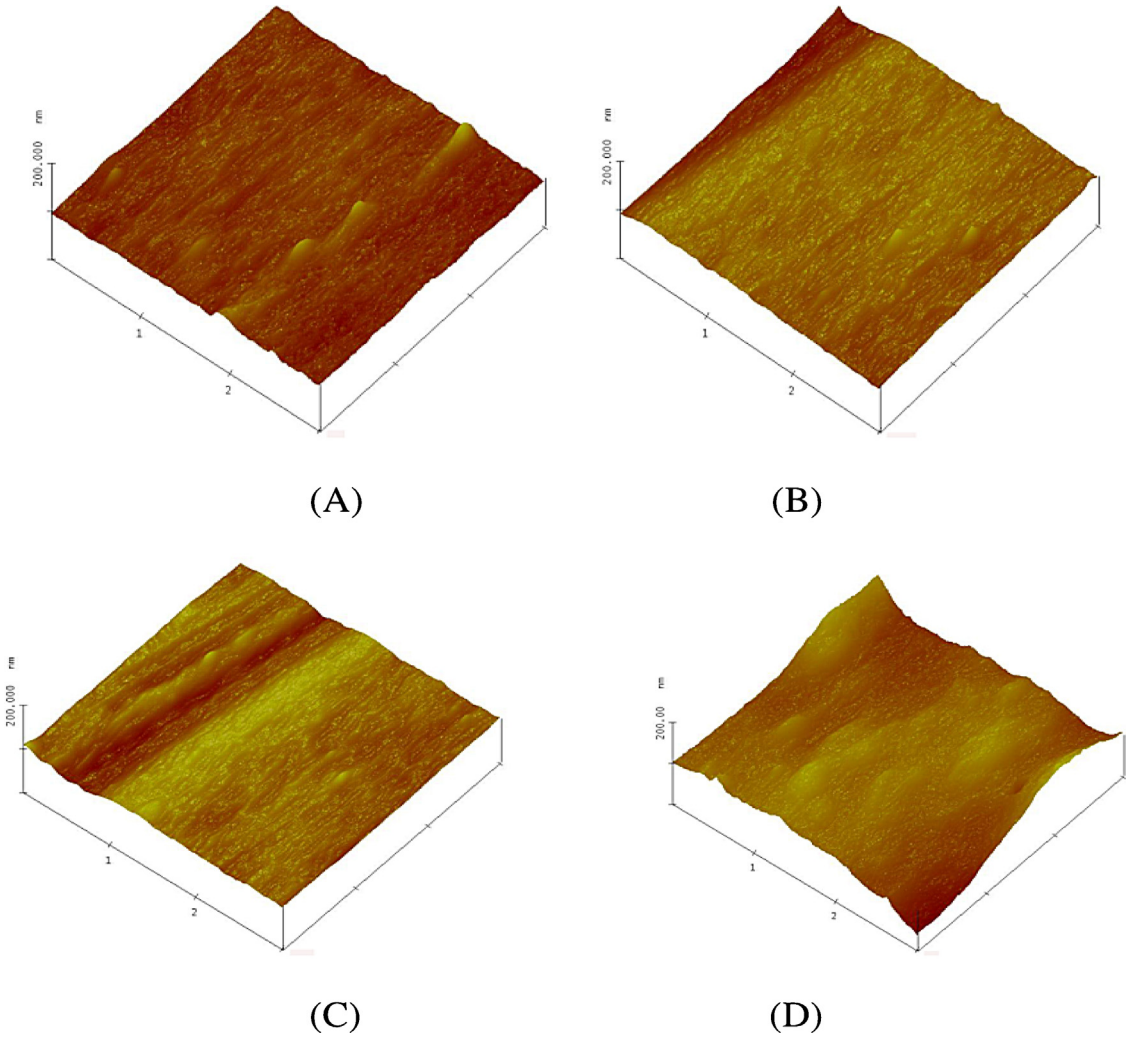

Fig. 7. AFM images of samples 25 (A, DS 0.06), 13 (B, DS 0.10), 26 (C, DS 0.14) and 27 (D, DS 0.55).

agreement with the DP determined from ^{1}H NMR. Besides the cross-correlations between f carbon with methylene protons in PCL chains, the primary cross-correlations were detected in Red colour at δ_C/δ_H 23.3/2.28 (C_b/H_a), 24.2/1.54 (C_b/H_d), 24.2/1.42 ($C_b/H_{d'}$), 24.2/1.30 (C_b/H_c), 25.1/2.34 (C_c/H_a), 25.3/1.54 ($C_c/H_{b,d}$), 25.3/1.42 ($C_c/H_{d'}$), 25.3/3.36 ($C_c/H_{e'}$), 25.3/4.00 (C_c/H_e), 31.9/1.56 ($C_{d,d'}/H_b$), 32.7/1.35 ($C_{d,d'}/H_c$), 31.9/3.36 ($C_{d'}/H_{e'}$), 34.2/1.56 (C_a/H_b), 34.2/1.30 (C_a/H_c), 61.2/1.42 ($C_{e'}/H_{d'}$), 61.2/1.30 ($C_{e'}/H_c$), and 63.5/1.54 ppm (C_e/H_d) confirming the correct assignments of primary carbon and proton signals in PCL side chains. In addition, the primary cross-correlations from AXU in xylan were also observed in Blue colour at 101.9/2.94 (C_1/H_2), 101.9/3.10 (C_1/H_5), 101.9/3.12 (C_1/H_3), 100.3/4.54 ($C_1/H_{2'}$), 76.3/3.27 (C_4/H_3), 76.7/4.42 ($C_4/H_{2'}$), 76.7/4.83 ($C_4/H_{3'}$), 73.9/3.53 (C_3/H_4), 73.9/3.13 (C_3/H_5), 73.9/2.96 (C_3/H_2), 72.4/3.27 (C_2/H_3), 72.0/4.85 ($C_2/H_{3'}$), 60.3/3.53 (C_5/H_4), and 60.3/3.26 ppm (C_5/H_3). The cross-correlations at δ_C/δ_H 101.9/3.54 (C_1/H_4) and 76.1/4.30 ppm (C_4/H_1) are associated with the linked xylose unit by β-1,4 linkage.

3.4. Thermal analysis

The thermal stability of regenerated xylan, xylan-*g*-PCL copolymers and the commercial PCL homopolymer was investigated by TGA and DTG, and the TGA/DTG curves are illustrated in Fig. 4.

In TGA curve, the weight loss prior to 150 °C was due to the removal of the absorbed moisture, which represents about 10% of the initial weight of regenerated xylan. Comparatively, this weight loss is marginal for the xylan-*g*-PCL copolymers due to the attachment of hydrophobic PCL side chains, while is negligible for the totally hydrophobic commercial PCL homopolymer (Fundador et al., 2012). Regenerated xylan began to decompose at about 188 °C, while xylan-*g*-PCL copolymer samples 26 (DS = 0.36) and 27 (DS = 1.39) began to decompose at 220 and 230 °C, respectively; at 50% weight loss, the decomposition temperature occurred at 238 °C for regenerated xylan, 269 for sample 26, and 274 °C for sample 27. These results indicated that the thermal stability of xylan-*g*-PCL copolymers increased after ROGP reaction. Comparatively, the commercial PCL homopolymer exhibited the extremely high thermal stability: it began to decompose at about 300 °C, and the decomposition temperature for 50% weight loss occurred at 376 °C. The relatively high thermal stability was probably due to the high DP and crystalline structure of the commercial PCL homopolymer.

DTG presents the weight loss rates and can be used for the comparison of the thermal stability between the samples (Nadji et al., 2009). In DTG curve, regenerated xylan and the commercial PCL homopolymer exhibited only one peak for the maximum degradation rate at 238 °C and 380 °C, respectively, while xylan-*g*-PCL copolymer samples 26 and 27 had two different peaks for the maximum degradation rate: the former peak for the degradation of xylan, and the latter for PCL side chains (Lönnberg, Fogelström, Berglund, Malmström, & Hult, 2008). Clearly, the second peak for

Table 2
Mechanical properties of the films produced from xylan-*g*-PCL copolymers.

Sample	DS	DP	Tensile stress (MPa)	Tensile strain at break (%)	Young's modulus (Mpa)
25	0.06	1.00	25.2 ± 4.8	4.2 ± 1.1	925 ± 44
13	0.10	1.07	20.9 ± 3.2	5.1 ± 1.8	764 ± 39
26	0.14	1.25	15.1 ± 2.7	6.4 ± 2.4	451 ± 31
27	0.55	1.53	9.8 ± 1.5	14.3 ± 2.5	225 ± 17

the degradation of PCL side chains increased with the improved DS. These data indicated that the thermal stability of xylan can be improved by the attachment of PCL, especially with the increased DS. However, in our previously report (Zhang et al., 2014), the thermal stability of xylan decreased upon ROGP reaction in DMSO/LiCl. The clearly different results were primary due to the different PCL side chains attached onto xylan. In DMSO/LiCl, only one ε-CL was attached onto xylan with each side chain, however, the length of PCL side chain substantially increased, which was probably responsible for the increased thermal stability due to the high thermal stability of PCL.

3.5. Film-forming property of xylan-g-PCL copolymers

Tensile strength of the films represents the maximum stress during tensile test and offers a measure of integrity and heavy-duty use potential of films. Table 2 presents the dependence of the mechanical properties, including the tensile stress, tensile strain at break and Young's modulus, on the DS of xylan-*g*-PCL films, and the typical stress–strain curves are shown in Fig. 5.

As shown in Table 2, with the increased DS, the tensile strength and the Young's modulus of the films decreased, while the elongation at break increased. Comparatively, sample 25 (DS 0.06, DP 1.00) showed the highest tensile strength (25.2 MPa) and a moderate tensile strain (4.2%), whereas sample 27 (DS 0.55, DP 1.53) had the highest elongation at break of 14.3%. This change was due to the presence of PCL side chains with a plasticizing effect which permits the film to be stretched to a certain extent (Lin & Lu, 2002).

3.6. Surface morphology of the films

The surface morphology of the xylan-*g*-PCL copolymer films was observed with SEM. Fig. 6 shows the representative SEM images. Comparatively, xylan-*g*-PCL copolymers with low DS had a uniform surface with less porous (Fig. 6A and B), while the surface became more highly porous with the increased DS and DP, which was probably due to the increased attachment of the PCL side chains onto xylan.

To further explore the surface morphology of the xylan-*g*-PCL films, AFM images of the films were collected and are illustrated in Fig. 7. A large difference in the structure of the grafted xylan with different DS was visualized. With the increased DS, the surface of films became to relatively more rough and showed larger nodules due to the attachment of PCL side chains.

4. Conclusions

The attachment of PCL onto xylan was accomplished in three kinds of dual polar aprotic solvents, including DMF/LiCl, DMAc/LiCl and NMP/LiCl. The effects of reaction parameters including the reaction media, reaction temperature and the molar ratio of ε-CL/AXU were investigated. The xylan derivatives with DS 0.01–0.55 and DP 1.00–1.54 were obtained under the selected conditions. FT-IR and NMR analyses provided the evidences of the chemical attachment of PCL side chains onto xylan. HSQC suggested that 13.04% and 86.96% of PCL side chains were attached to C_2 and C_3 positions of AXU, respectively. The thermal stability of xylan increased upon ROGP reaction due to the increased length of PCL side chains. The increased film-forming properties of xylan derivatives were confirmed. SEM and AFM observations provided the evidences of the increased film properties due to the attachment of PCL side chains.

Acknowledgements

This work was financially supported by the National Natural Science Foundation of China (31170550, 31170555), Program for New Century Excellent Talents in University (NCET-11-0154), the Fundamental Research Funds for the Central Universities (2014ZG0046), and the National Program for Support of Top-notch Young Professionals.

References

Belmokaddem, F. Z., Pinel, C., Huber, P., Petit Conil, M., & Da Silva Perez, D. (2011). Green synthesis of xylan hemicellulose esters. *Carbohydrate Research*, *346*, 2896–2904.
Cao, X. F., Sun, S. N., Peng, X. W., Zhong, L. X., & Sun, R. C. (2013). Synthesis and characterization of cyanoethyl hemicelluloses and their hydrated products. *Cellulose*, *20*, 291–301.
Carlmark, A., Larsson, E., & Malmström, E. (2012). Grafting of cellulose by ring-opening polymerisation – A review. *European Polymer Journal*, *48*, 1646–1659.
Dupont, A. L. (2003). Cellulose in lithium chloride/N,N-dimethylacetamide, optimisation of a dissolution method using paper substrates and stability of the solutions. *Polymer*, *44*, 4117–4126.
Edgar, K. J., Arnold, K. M., Blount, W. W., Lawniczak, J. E., & Lowman, D. W. (1995). Synthesis and properties of cellulose acetoacetates. *Macromolecules*, *28*, 4122–4128.
El Seoud, O. A., Marson, G. A., Ciacco, G. T., & Frollini, E. (2000). An efficient, one-pot acylation of cellulose under homogeneous reaction conditions. *Macromolecular Chemistry and Physics*, *201*, 882–889.
Fundador, N. G. V., Enomoto-Rogers, Y., Takemura, A., & Iwata, T. (2012). Syntheses and characterization of xylan esters. *Polymer*, *53*, 3885–3893.
Gross, A. S., Bell, A. T., & Chu, J.-W. (2013). Preferential interactions between lithium chloride and glucan chains in N,N-dimethylacetamide drive cellulose dissolution. *The Journal of Physical Chemistry B*, *117*, 3280–3286.
Guo, Y. Z., Wang, X. H., Shen, Z. G., Shu, X. C., & Sun, R. C. (2013). Preparation of cellulose-graft-poly(epsilon-caprolactone) nanomicelles by homogeneous ROP in ionic liquid. *Carbohydrate Polymers*, *92*, 77–83.
Habibi, Y., Goffin, A.-L., Schiltz, N., Duquesne, E., & Dubois, P. (2008). Bionanocomposites based on poly(ε-caprolactone)-grafted cellulose nanocrystals by ring-opening polymerization. *Journal of Materials Chemistry*, *18*, 5002–5010.
Hansen, N. M. L., & Plackett, D. (2008). Sustainable films and coatings from hemicelluloses: a review. *Biomacromolecules*, *9*, 1493–1505.
He, X., Liang, L., Xie, M., Zhang, Y., Lin, S., & Yan, D. (2007). Synthesis of novel linear PEO-b-PS-b-PCL triblock copolymers by the combination of ATRP, ROP, and a click reaction. *Macromolecular Chemistry and Physics*, *208*, 1797–1802.
Lönnberg, H., Fogelström, L., Berglund, L., Malmström, E., & Hult, A. (2008). Surface grafting of microfibrillated cellulose with poly(ε-caprolactone) – Synthesis and characterization. *European Polymer Journal*, *44*, 2991–2997.
Lönnberg, H., Zhou, Q., Brumer, H., Teeri, T. T., Malmström, E., & Hult, A. (2006). Grafting of cellulose fibers with poly(ε-caprolactone) and poly(l-lactic acid) via ring-opening polymerization. *Biomacromolecules*, *7*, 2178–2185.
Labet, M., & Thielemans, W. (2011). Improving the reproducibility of chemical reactions on the surface of cellulose nanocrystals: ROP of ε-caprolactone as a case study. *Cellulose*, *18*, 607–617.
Lin, W. J., & Lu, C. H. (2002). Characterization and permeation of microporous poly(ε-caprolactone) films. *Journal of Membrane Science*, *198*, 109–118.
Malmstrom, E., & Carlmark, A. (2012). Controlled grafting of cellulose fibres – An outlook beyond paper and cardboard. *Polymer Chemistry*, *3*, 1702–1713.
Marianne Labet, W. T. (2011). Citric acid as a benign alternative to metal catalysts for the production of cellulose-grafted-polycaprolactone copolymers. *Polymer Chemistry*, 6.

Nadji, H., Diouf, P. N., Benaboura, A., Bedard, Y., Riedl, B., & Stevanovic, T. (2009). Comparative study of lignins isolated from alfa grass (*Stipa tenacissima* L.). *Bioresource Technology*, *100*, 3585–3592.

Saha, B. (2003). Hemicellulose bioconversion. *Journal of Industrial Microbiology and Biotechnology*, *30*, 279–291.

Sinha, V. R., Bansal, K., Kaushik, R., Kumria, R., & Trehan, A. (2004). Poly-ε-caprolactone microspheres and nanospheres: an overview. *International Journal of Pharmaceutics*, *278*, 1–23.

Striegel, A. (1997). Theory and applications of DMAC/LICL in the analysis of polysaccharides. *Carbohydrate Polymers*, *34*, 267–274.

Stryuk, S., Eckelt, J., & Wolf, B. (2005). Solutions of cellulose in DMAc + LiCl: migration of the solute in an electrical field. *Cellulose*, *12*, 145–149.

Sun, R., Fang, J. M., & Tomkinson, J. (2000). Stearoylation of hemicelluloses from wheat straw. *Polymer Degradation and Stability*, *67*, 345–353.

Sun, R. C., & Tomkinson, J. (2002). Characterization of hemicelluloses obtained by classical and ultrasonically assisted extractions from wheat straw. *Carbohydrate Polymers*, *50*, 263–271.

Sun, S. N., Li, M. F., Yuan, T. Q., Xu, F., & Sun, R. C. (2012). Effect of ionic liquid pretreatment on the structure of hemicelluloses from corncob. *Journal of Agricultural and Food Chemistry*, *60*, 11120–11127.

Takaragi, A., Minoda, M., Miyamoto, T., Liu, H., & Zhang, L. (1999). Reaction characteristics of cellulose in the LiCl/1,3-dimethyl-2-imidazolidinone solvent system. *Cellulose*, *6*, 93–102.

Wang, H. T., Yuan, T. Q., Meng, L. J., She, D., Geng, Z. C., & Sun, R. C. (2012). Structural and thermal characterization of lauroylated hemicelluloses synthesized in an ionic liquid. *Polymer Degradation and Stability*, *97*, 2323–2330.

Wang, Z., Zheng, L., Li, C., Zhang, D., Xiao, Y., Guan, G., et al. (2013). A novel and simple procedure to synthesize chitosan-graft-polycaprolactone in an ionic liquid. *Carbohydrate Polymers*, *94*, 505–510.

Williamson, S. L., Armentrout, R. S., Porter, R. S., & McCormick, C. L. (1998). Microstructural examination of semi-interpenetrating networks of poly(N,N-dimethylacrylamide) with cellulose or chitin synthesized in lithium chloride/N,N-dimethylacetamide. *Macromolecules*, *31*, 8134–8141.

Xie, W., Chen, D., Fan, X., Li, J., Wang, P. G., Cheng, H. N., et al. (1999). Lithium chloride as catalyst for the ring-opening polymerization of lactide in the presence of hydroxyl-containing compounds. *Journal of Polymer Science Part A: Polymer Chemistry*, *37*, 3486–3491.

Xu, Q., Kennedy, J. F., & Liu, L. (2008). An ionic liquid as reaction media in the ring opening graft polymerization of ε-caprolactone onto starch granules. *Carbohydrate Polymers*, *72*, 113–121.

Zhang, X. Q., Chen, M. J., Liu, C. F., & Sun, R. C. (2014). Dual-component system dimethyl sulfoxide/LiCl as a solvent and catalyst for homogeneous ring-opening grafted polymerization of ε-caprolactone onto xylan. *Journal of Agricultural and Food Chemistry*, *62*, 682–690.